Synthesis and characterization of carboxylated thiophene co-polymers and their use in photovoltaic cells

Article *in* Current Science · September 2008

CITATIONS
5

READS
218

2 authors:

Roshan Fernando
Colorado School of Mines
22 PUBLICATIONS **378** CITATIONS
SEE PROFILE

G.K.R. Senadeera
National Institute of Fundamental Studies - Sri Lanka
122 PUBLICATIONS **1,945** CITATIONS
SEE PROFILE

Synthesis and characterization of carboxylated thiophene co-polymers and their use in photovoltaic cells

J. M. R. C. Fernando and G. K. R. Senadeera*

Institute of Fundamental Studies, Hantane Road, Kandy, Sri Lanka

Several 3-substituted thiophene and pyrole ring-bearing co-polymers was chemically synthesized and their possible usage as sensitizers was investigated by fabricating solar devices with mesoporous TiO_2 electrodes and a redox liquid electrolyte containing I_3^-/I^-. Monomers of 3-thiophene acetic acid (3TAA), 3-thiophene malonic acid (3TMA), 3-methyl thiophene (3MT), thiophene (T), 3-acetyl thiophene (3AT) and pyrrole (PY) were used as starting materials to obtain their co-polymers. The photocells were able to generate reasonably high photocurrent with the addition of ionic liquid 1-methyl-3-*n*-hexylimidazolium iodide to the electrolyte. The corresponding values obtained for short-circuit current densities and efficiencies of the cells sensitized with poly 3TAA, poly 3TAA–poly 3TMA, poly 3TAA–poly 3MT, poly 3TAA–poly 3AT, poly 3TAA–poly T and poly 3TAA–poly PY were 4.35, 3.29, 3.12, 2.97, 2.25, 1.85 mA cm^{-2} and 1.2, 0.76, 0.76, 0.51, 0.42, 0.41 respectively.

Keywords: Co-polymers, characterization, synthesis, photovoltaic cells.

THE search for substitutes of fossil-energy sources and the growing environmental awareness worldwide have strengthened interest in photovoltaics as long-term available, cheap, environmental-friendly and reliable energy technology. Titanium dioxide-based dye-sensitized solar cells (DSCs) developed in the 1990s, are a non-conventional solar electric technology that has attracted much attention[1–6], perhaps as a result of its record efficiency above 10%.

One of the problems associated with these solar cells is the use of expensive sensitizers containing rare earth metal complexes, such as ruthenium(II) polypyridyl complexes. Due to their high cost and long-term unavailability, investigations have widened to search for low-cost, efficient sensitizers. In this context, inexpensive conductive polymer (CP) materials, which could behave either as sensitizers or hole conductors, are of practical interest as possible replacement for the liquid electrolyte and/or the sensitizers in these devices[3,7–16]. However, insolubility, infusibility and air-instability of this class of polymers restricted their use in semiconducting devices, especially in solar cells. On the other hand, the availability of suitable energy levels of CPs, which ensures that electron injection from the excited dye molecules into the conduction band of TiO_2 is thermodynamically possible and the rigid attachment between the polymer and the surface of the semiconductor via chemical bonding are crucial factors effecting the efficiency of these devices. Therefore, one of the challenges in devising these cells is the identification of suitable carboxylated polymers with the requisite properties, such as wide absorption (panchromatic), appropriate band gap, band positions and methods for their deposition. In this context, we have recently explored the possibilities of using conducting polymers with carboxylic groups as efficient sensitizers, specially with poly(3-thiophene acetic acid), in DSCs and have observed unusually high photocurrent yields in the systems based on conducting polymers[12–16].

Our strategies towards higher efficiencies in these conjugated polymer-sensitized TiO_2 solar cells are basically twofold. One is the improvement in surface contacts between the sensitizing polymer molecules with the mesoporous TiO_2 surface and the second is the expansion of spectral response of the CPs to the near-IR region. With respect to spectral expanding, it is established that the absorption maxima and the band gap of these CPs, depend on the length of the conjugation of a polymer. Therefore, either a red shift or blue shift can be obtained by varying the conjugation length. The length of the conjugation can be varied in different ways. The most popular method is to use different co-polymers with conjugated and non-conjugated segments. Co-polymerization of different monomers to give regio-specific polymers has also been attempted.

Therefore, in order to obtain panchromatic carboxylated conducting polymer, we have chosen to control the conjugation along the polymer backbone by synthesizing co-polymers with 3-thiophene acetic acid (3TAA). In this study we have chosen some commercially available, relatively inexpensive monomers [thiophene malonic acid (3TMA), thiophene (T), 3-acetyl thiophene (3AT), 3-methyl thiophene (3MT) and pyrrole (PY)] and synthesized their co-polymers with 3TAA. Photoresponses of the above polymers were examined by fabricating solar cells

*For correspondence. (e-mail: rsena@ifs.ac.lk)

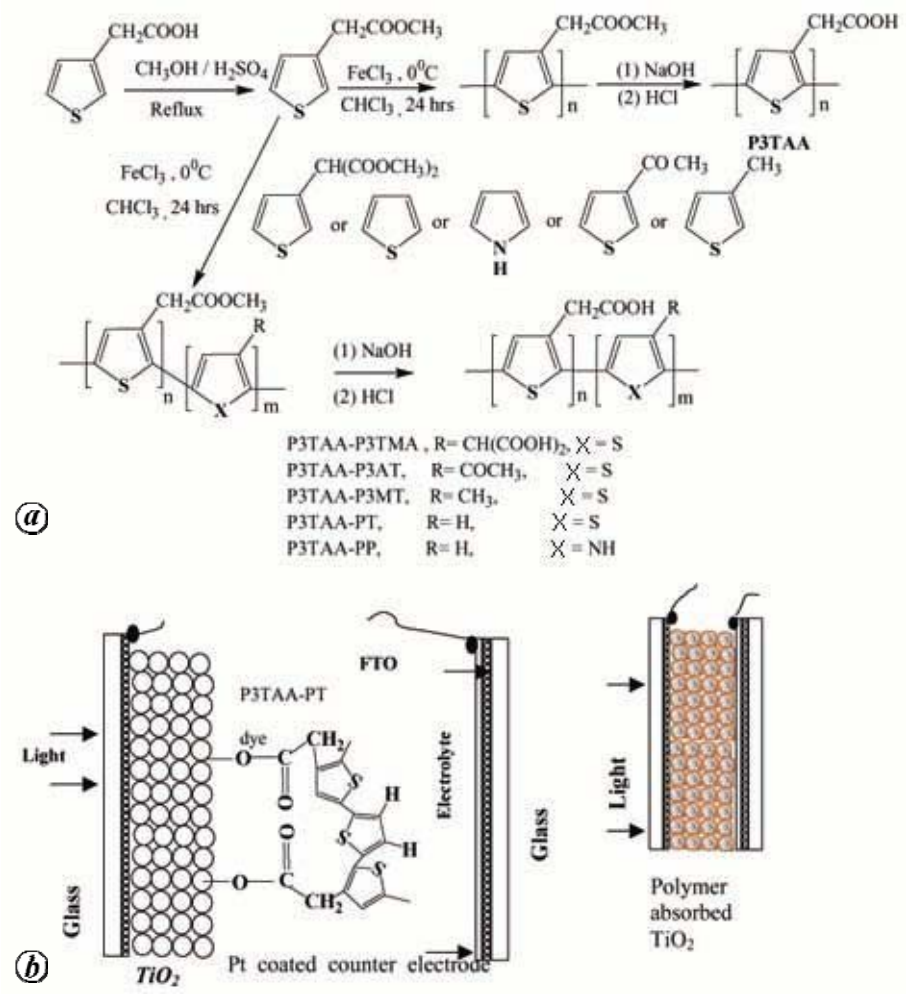

Figure 1. Schematic diagram of (***a***) synthesis of P3TAA and other polymers and (***b***) fabrication of polymer-sensitized devices.

comprising mesoporous TiO_2. These polymers have high solubility in organic solvents with different spectral responses and to be adhere well to the mesoporous TiO_2 surface on penetration into the labyrinthine spaces. In addition, based on our previous observations that the imidazolium cations strongly adsorbed on the TiO_2 surface, enhancing the electron diffusion in mesoporous TiO_2 electrodes[17,18], we have successfully employed an ionic liquid, 1-methyl-3-*n*-hexylimidazolium iodide (MHImI) in the present devices, observing an enhancement in the performances of these solar cells.

Experimental

Polymerization of 3TAA

Poly(3-thiophene acetic acid) (P3TAA) was synthesized as described by Kim *et al*. (Figure 1 *a*)[11]. Ten grams of 3TAA (Nacali Tesque, Japan) was refluxed for 24 h with acidified H_2SO_4 (five drops), dehydrated methanol (50 ml; Wako, Japan) to protect the carboxylic acid moiety of the monomer from oxidative decomposition. Methanol was then evaporated using a rotary evaporator and diethyl ether was used to extract the residue. The extract was thoroughly washed with sufficient amount of deionized water, dried with anhydrous $MgSO_4$ and filtered. After the rotary evaporation of diethyl ether, 3TMA was recovered and checked by ^{1}H NMR (JEOL EX-270, 270 MHz). For chemical polymerization of the monomer, 10 mmol anhydrous ferric chloride (Wako) dissolved in dehydrated chloroform (75 ml; Wako) was used under N_2 atmosphere at 0°C in a three-necked flask and kept under stirring. Drop-wise addition of the protected monomer, 3-thiophene methyl acetate (3TMACE, 1 mmol) dissolved in dehydrated chloroform ($CHCl_3$; 50 ml) was carried out under the above conditions. After 12 h of polymerization, brown-red coloured poly 3TMA (P3TMA) was precipitated by adding the above polymerized solution to a large excess of methanol (1 l) and the residual oxidant and the oligomeres were removed by repeated washing with fresh methanol and deionized water. Hydrolysis was carried out by heating P3TMA (0.5 g) in 50 ml of 2.0 M NaOH

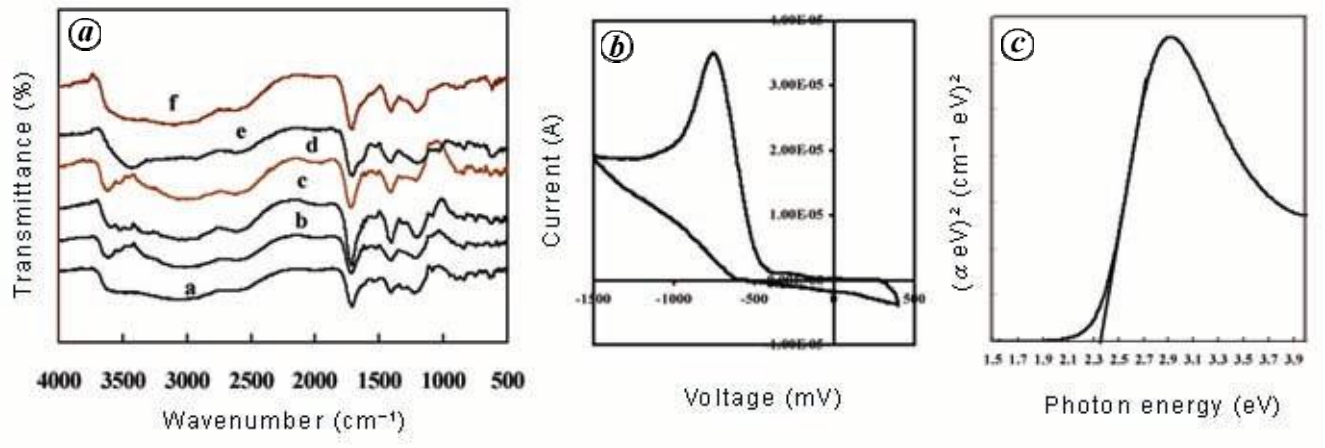

Figure 2. ***a***, FT-IR spectra of polymers (a) P3TAA, (b) P3TAA–PP, (c) P3TAA–P3AT, (d) P3TAA–P3TMA, (e) P3TAA–P3MT and (f) P3TAA–PT. ***b***, Cyclic voltammogram of P3TAA in $LiClO_4$/acetonitile vs Ag/AgCl reference electrode. ***c***, Optical density of P3TAA film.

solution for 24 h and the mixture was filtered to remove the insoluble part. The water-soluble part was neutralized and precipitated using dilute HCl solution. The precipitate was carefully washed with deionized water by high speed centrifuging and vacuum-dried for 24 h (yield 75%). FT-IR spectra of P3TAA and 3TMACE were compared using Perkin Elmer system 2000 FT-IR spectrometer (Figure 2 *a*; KBr, 2400–3600 cm^{-1} (broad)), O–H stretching, C–H stretching on thiophene ring and aliphatic CH_2 1725 cm^{-1}, C=O stretching, 1300 cm^{-1}, C–O stretching, 1414 cm^{-1} and 931 cm^{-1}, C–O–H, bending 1464 cm^{-1}, thiophene ring stretching (symmetric), 1630 cm^{-1}, asymmetric ring stretching. Formation of P3TAA was reconfirmed by ^{1}H NMR (JEOL EX-270, 270 MHz) in dimethyl sulfoxide (DMSO; Figure 3 *A*), δ 12.53 ppm (*s*, –COOH, 1H), 7.49–7.28 ppm (*m*, thiophene ring proton, 1H), 3.78–3.35 ppm (*m*, $–CH_2–$, 2H).

Polymerization of P3TAA–P3TMA

Co-polymer was synthesized according to the method described in Figure 1. A mixture of monomers (10 mmol), 3TMACE (8 mmol) and TMA (2 mmol) dissolved in dried $CHCl_3$ (20 ml) was added drop-wise to a solution of anhydrous $FeCl_3$ (40 mmol) in dried $CHCl_3$ (30 ml) in a three-necked flask (250 ml) at 0°C, under N_2 atmosphere. The mixture was then stirred for 24 h under the same condition. After the reaction, the mixture was poured into a large excess of methanol to precipitate the polymer. The precipitate was filtered and washed with distilled water. Hydrolysis and precipitation of co-polymer were carried out according to the method described in previous cases (yield 51%). ^{1}H NMR was used to confirm the existence of co-polymer (Figure 3 *b*); δ 12.53 ppm (*s*, –COOH, 1H), 7.49–7.28 ppm (*m*, thiophene ring proton, 1H), 5.13 ppm (*m*, thiophene ring –CH–, H), 3.78–3.35 ppm (*m*, thiophene ring $–CH_2–$, 2H), and FT-IR 2400–3600 cm^{-1} (broad), O–H stretching, C–H stretching on thiophene ring and aliphatic CH_2, 1723 cm^{-1}, C=O stretching (carboxylic), 1260 cm^{-1}, C–O stretching, 1416 cm^{-1} and 943 cm^{-1}, C–O–H bending, 1466 cm^{-1}, thiophene ring stretching (symmetric), 1625 cm^{-1}, asymmetric ring stretching (Figure 2 *a*).

Polymerization of poly 3TAA–polythiophene

As in the previous case a mixture of monomers (Figure 1 *a*), 3 TMACE (8 mmol) and T (2 mmol) was dissolved in dried $CHCl_3$ (20 ml) and the aforementioned method was followed to obtain P3TAA–polythiophene (PT) (yield 46%). ^{1}H NMR was used to elucidate the existence of co-polymer. In DMSO, δ 12.53 ppm (*s*, –COOH, 1H), 7.54–7.28 ppm (*m*, thiophene ring proton, 1H), 3.78–3.35 ppm (*m*, $–CH_2–$, 2H; Figure 3 *C*). 2400–3600 cm^{-1} (broad), O–H stretching, C–H stretching on thiophene ring and aliphatic CH_2, 1704 cm^{-1}, C=O stretching (carboxylic), 1286 cm^{-1}, C–O stretching, 1406 cm^{-1} and 936 cm^{-1}, C–O–H bending, 1424 cm^{-1}, thiophene ring stretching (symmetric), 1625 cm^{-1}, asymmetric ring stretching (Figure 2 *a*).

Polymerization of P3TAA–polypyrrole

A mixture of monomers, 3TMACE (8 mmol) and PY (2 mmol) was dissolved in dried $CHCl_3$ (20 ml) and co-polymer was obtained as in the previous case (yield 35%). ^{1}H NMR data confirmed the co-polymerization. In DMSO, δ 12.56 ppm (*s*, –COOH, 1H), δ 8.3 ppm (NH), 7.49–7.28 ppm (*m*, thiophene ring proton, 1H), 6.8 ppm (*d* pyrrole ring 1 H), 3.78–3.35 ppm (*m*, $–CH_2–$, 2H) (Figure 2). 2400–3600 cm^{-1} (broad), O–H stretching, C–H stretching on thiophene ring and aliphatic CH_2, 3492 cm^{-1}, N–H stretching (pyrrole ring), 1708 cm^{-1}, C=O stretching (carboxylic), 1289 cm^{-1}, C–O stretching, 1422 cm^{-1} and 952 cm^{-1}, C–O–H bending, 1464 cm^{-1}, thio-

phene ring stretching (symmetric), 1630 cm^{-1}, asymmetric ring stretching (Figure 2 *a*).

Polymerization of P3TAA–poly(3MT)

A mixture of monomers, 3TMACE (8 mmol) and 3MT (2 mmol) was dissolved in dried $CHCl_3$ (20 ml) and co-polymer was obtained as in the previous case (yield 54%). ^1H NMR measurements confirmed the existence of co-polymer giving following values in DMSO: δ 12.63 ppm (*s*, –COOH, 1H), 7.30 ppm (*m*, thiophene ring proton, 1H), 3.80 ppm (*m*, $–CH_2$), 3.54 ppm ($C–CH_3$, 3H; Figure 3 *e*). 2400–3600 cm^{-1} (broad), O–H stretching, C–H stretching on thiophene ring and aliphatic CH_2 and CH_3, 1720 cm^{-1}, C=O stretching (carboxylic), 1266 cm^{-1}, C–O stretching, 1437 cm^{-1} and 917 cm^{-1}, C–O–H bending, 1461 cm^{-1}, thiophene ring stretching (symmetric), 1625 cm^{-1}, asymmetric ring stretching (Figure 2 *A*).

Polymerization of P3TAA–poly(3AT)

A mixture of monomers, 3TMACE (8 mmol) and 3AT (2 mmol) was dissolved in dried $CHCl_3$ (20 ml) and co-polymer was obtained as in the previous case (yield 54%). ^1H NMR was used to confirm the existence of co-polymer. In DMSO, δ 12.65 ppm (*s*, –COOH, 1H), δ 8.17 ppm δ (thiophene ring proton, 1H), 7.35 ppm (thiophene ring proton 1H), 3.68 ppm (*m*, $C=O–CH_3$) 3.82 ppm (*d*, CH_2; Figure 3 *f*). 2400–3600 cm^{-1} (broad), O–H stretching, C–H stretching on thiophene ring and aliphatic CH_2 and CH_3, 1713 cm^{-1}, C=O stretching (carboxylic), 1673 cm^{-1}, C=O stretching (acetyl), 1285 cm^{-1}, C–O stretching, 1403 cm^{-1} and 944 cm^{-1}, C–O–H bending, 1459 cm^{-1}, thiophene ring stretching (symmetric), 1626 cm^{-1}, asymmetric ring stretching (Figure 2 *a*).

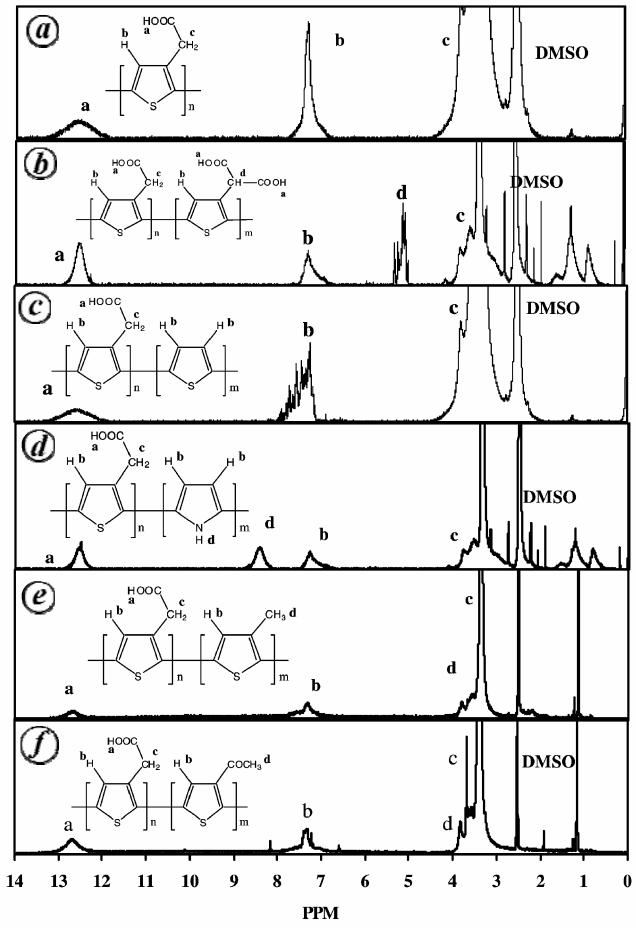

Figure 3. ^1H NMR data obtained for the polymers.

Characterization of polymers

Optical absorption measurements were carried out with a Shimadzu dual wavelength/double beam spectrophotometer (model UV-3000). The highest occupied molecular orbital (HOMO), lowest unoccupied molecular orbital (LUMO) and the band-gap values of polymers were calculated using cyclic voltammograms and UV–visible absorption measurements, according to the method described elsewhere[9,10].

Fabrication of photoelectrochemical cells

Mesoporus TiO_2 films were deposited on pre-cleaned, fluorine-doped conducting tin oxide (FTO) glasses (Nippon sheet glass, 10–12 Ohm sq^{-1}) by spraying a solution of TiO_2 prepared as follows: TiO_2 (Aerosil, P-25, 0.5 g) was added to a mortar containing 50 drops (2 ml) of acetic acid and ground well for 1 min. Then 0.5 ml of titanium tetra-1-methylethoxide was added. The mixture was ground and 0.1 ml of deionized water was added to it. Surfactant Triton X-100 (Aldrich) was added (0.1 ml) and mixture was ground thoroughly. Ethanol (100 ml) was then added to the mixture and sonicated for 10 min. Finally the solution was further diluted using ethanol (1 : 4 v/v) and sprayed onto the preheated glass substrates which were placed on a digital hotplate at 300 ± 5°C. The electrodes were then sintered at 500°C for 1 h and average thicknesses was ~4 μm. The thickness of the films on FTO substrates was determined using Dektak profilometer (Veeco, Dektack 3). The above confirmed polymers were dissolved in dried DMSO. TiO_2 electrodes were dipped in the respective polymer solution at least for 24 h and washed either with dried THF or ethanol and dried under N_2. Photoelectrochemical cells were constructed by introducing the redox electrolyte containing tetrabutylammonium iodide (0.5 M)/I_2 (0.05 M), in a mixture of acetonitrile and ethylene carbonate (6 : 4 v/v) between the polymer-coated TiO_2 electrodes and Pt-coated counter electrode as shown in Figure 1 *b*. After measuring the photoresponses of these cells, a drop (1/8 ml) of 0.5 M

MHImI solution in acetonitrile (5 ml) was introduced to the cells and the photo-responses were remeasured.

Solar-cell characterization

Current–voltage (*I–V*) characteristics of the cell were examined with a standard solar irradiation of 100 mW cm^{-2} (Xe-lamp with an Orial AM 1.5 filter) as the light source. An Eko pyranometer was used to measure light intensity. A fully computerized set-up consisting of multimeter (Keithley 2000) coupled to potentiostat (Hokuto Denko, HA 301) via a computer was used for data acquisition. The power conversion efficiency (η) was calculated according to the following equation: $\eta = \mathrm{FF} \times J_{sc} \times V_{oc}/I$, where J_{sc} is the short-circuit photocurrent density (A cm^{-2}), V_{oc} the open-circuit voltage (V), I the intensity of the incident light (W cm^{-2}) and FF the fill factor defined as $\mathrm{FF} = J_m V_m / J_{sc} V_{oc}$, where J_m and V_m are the optimum photocurrent and voltage that can be extracted from the maximum power point of the *I–V* characteristics[1,2,12,19]. The effectiveness of the cell to convert light of various wavelengths into electrical current was measured as the incident photon to current conversion efficiency (IPCE) defined as the number of electrons generated by light per number of photons incident on the cell, formulated by $\mathrm{IPCE}\% = 1240 J_{sc}/\lambda W_i$, where J_{sc} is the short-circuit current density (μA cm^{-2}), λ the excitation wavelength (nm) and W_i is the photon flux (W m^{-2})[1,10,12,19], using a Nikon monochromator auto-scanner ASC-1101 coupled to a Keithley multimeter via a computer. The measured photocurrent spectra were corrected for the spectral response of the lamp and monochromator by normalization to the response of a calibrated silicon photodiode (Hamamatsu, model S 1227 1010BQ), whose sensitivity spectrum was known. No correction was made for reflection off the surface of the sample. The effective cell area was 0.25 cm^2 and a mask was used to keep the cell area constant during all *I–V* measurements.

Results and discussion

As can be seen from Figure 2 *a*, for all polymers FT-IR spectra show broad absorption between 2400 and 3600 cm^{-1}. This may include O–H stretching, heteroaromatic C–H stretching and aliphatic C–H stretching. Further, the absorption intensities are higher between 2900 and 3600 cm^{-1}. This must be due to the increased number of free O–H groups on the polymer chain. Therefore, it provides an evidence for the presence of more head-to-tail (HT–HT) linkages of polymers[20–23]. Because HT–HT arrangements reduces hydrogen bonding between carboxylic groups and therefore cause an increase in the number of free hydroxyl groups on the polymer chain. Another clear evidence in the IR spectra for HT–HT arrangements and longer conjugation of polymers, is the intensity ratio of the symmetric ring stretch at ~1460 cm^{-1} to the asymmetric ring stretch at ~1625 cm^{-1} (I_{sym}/I_{asym})[22,23]. This ratio is smaller for polymers with long conjugation length. Since the polymer we synthesized showed a ratio around 1, it can be concluded that these polymers have longer conjugation length[22,23].

Figure 3 shows the ^{1}H NMR spectra of the polymers synthesized in the present study. The ^{1}H NMR spectra of P3TAA show a single peak at 7.29 ppm for the aromatic proton in the thiophene ring (Figure 3 *a*). This is an indication for the regioregular HT–HT arrangement of the polymer chain as shown in Figure 4 *a*(a). If the polymer has an arrangement as shown in Figure 4 *a*(b) or any other irregular arrangement, the respective NMR peak must show a splitting pattern. A similar phenomenon has been observed in earlier studies by several groups on 3-alkyl thiophenes[22,23]. However, while co-polymers P3TAA–P3TMA, P3TAA–P3MT and P3TAA–P3AT show splitting patterns, co-polymer P3TAA–P3TMA has a signal between 6.70 and 7.50 ppm. Even though most of the co-polymers show splitting patterns in their respective NMR spectra, it is not possible to predict whether they are region-random. Because, this splitting may be due to presence of two or three aromatic protons in the co-polymers. Co-polymers P3TAA–PT and P3TAA–PPY show good splitting patterns. This is because in the co-

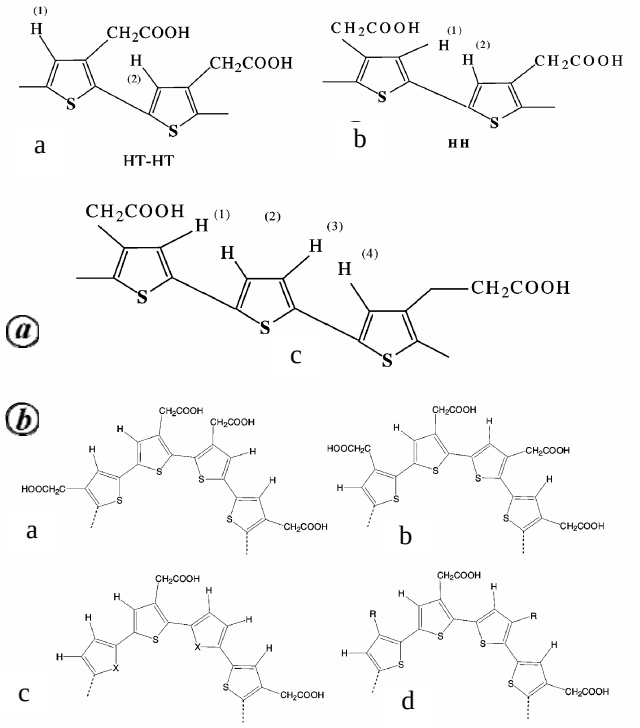

Figure 4. ***a***, Possible arrays of co-polymers. ***b***, Chemical structures of polymers (a) P3TAA (HH–TT), (b) P3TAA (HT–HT), (c) P3TAA–PT and P3TAA–PP and (d) P3TAA–P3TMA, P3TAA–P3AT and P3TAA–P3MT.

polymer aromatic proton can couple regardless of the arrangement. Therefore, in general this splitting behaviour can be regarded as evidence for the co-polymerization as depicted in the Figure 4 *b*. UV–visible absorption spectra of polymer dyes in DMSO and the IPCE are depicted in Figure 5 *a*. While the absorption spectrum of the polymer P3TAA in DMSO (curve i) showed an intense absorption at ~417 nm, P3TAA–P3TMA and P3TAA–PPy polymers showed intense bands at ~426 nm (curve iii) and ~420 nm (curve iv) respectively. Co-polymers P3TAA–P3MT, P3TAA–P3AT and P3TAA–PT showed maximum absorption peaks at ~415 nm (curve ii), 411 nm (curve v) and ~391 nm (curve vi) respectively. Even though we have synthesized these polymers expecting more red shift in the absorption, neither the shift in the maximum absorption nor the expansion in the spectral response was large enough as we had expected. While curves curves (a)–(f) in Figure 5 *b* show the IPCE values of cells sensitized with P3TAA, P3TAA–P3MT, P3TAA–P3TMA, P3TAA–PPy, P3TAA–P3AT and P3TAA–PT respectively, curve (g) shows the IPCE values for the bare TiO_2 film with the electrolyte. As can be seen in Figure 5 *a* and *b*, the close relationship and the red shifts of the action spectra with the optical absorption spectra indicate that the photoelectrochemical conversion is achieved through photosensitization, namely that polymer molecules absorbed photons and generated excited electrons, and the excited electrons were subsequently transferred to the conduction band of the TiO_2 electrode.

In order to thermodynamically judge the possibilities of electron transfer from the excited dye molecules to the conduction band of TiO_2, HOMO levels of the polymers were estimated. As an example, Figure 2 *b* shows the cyclic voltammogram of P3TAA. The onset potential for the oxidation of P3TAA determined from the graph was 0.65 vs NHE (0.43 vs Ag/AgCl). The HOMO energy level that is essentially the ionization of the polymer could be determined using an empirical relation $qV_{onset} + 4.4$ eV, where V_{onset} is the onset potential vs standard calomel electrode (SCE). Hence the determined energy level for the HOMO of P3TAA was 5.29 eV vs vacuum (recall that SCE is 0.24 V NHE, Ag/AgCl is 0.22 V vs NHE and 0 V vs NHE = 4.5 eV vs vacuum). Since the UV–visible absorbance measurements can be used to estimate the energy levels of the unoccupied molecular orbital (LUMO) of the polymers, the optical densities of polymers were plotted by assuming that the polymers possess a direct band gap. Figure 2 *c* depicts the corresponding optical density of P3TAA. According to the graph, the calculated value for the band gap of P3TAA was 2.39 eV and hence the evaluated value of LUMO for P3TAA was 2.99 eV. The other evaluated values of the HOMO and LUMO energy levels of the synthesized polymers are given in Table 1. As can be seen from Table 1, the excited state energy levels for the polymers are higher than the energy level of TiO_2 conduction band edge (–4.40 eV)[1,2,19] showing that the electron injection should be possible thermodynamically. Therefore, upon illumination of the cell, polymer dyes absorb light and get excited from the HOMO level to the LUMO level and eject electrons to the conduction band of TiO_2, which transports these electrons to the transparent bottom electrode (FTO) and then to the other end of the cell via external load and being received by the redox mediator (I_3^-/I^-) in the electrolyte. Finally the electrolyte (I_3^-/I^-) regenerates the polymers to their ground state, completing the cell reaction.

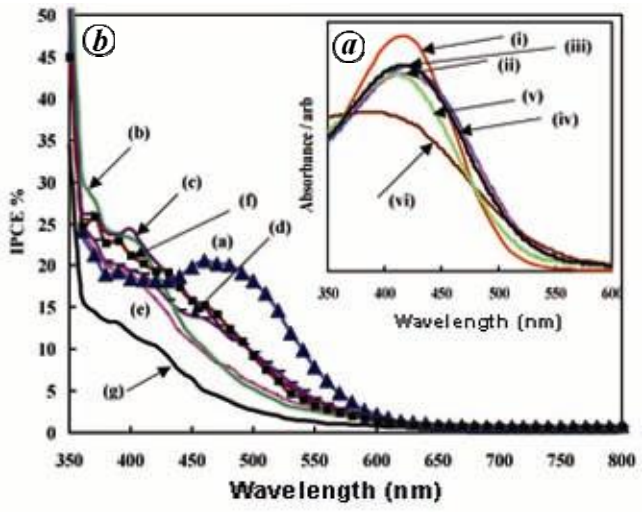

Figure 5. ***a***, UV–visible absorption spectra of polymer dyes in DMSO. (i) P3TAA, (ii) P3TAA–P3MT, (iii) P3TAA–P3TMA, (iv) P3TAA–PPy, (v) P3TAA–P3AT, (vi) P3TAA–PT. ***b***, IPCE values of cells sensitized with (a) P3TAA, (b) P3TAA–P3MT, (c) P3TAA–P3TMA, (d) P3TAA–PPy, (e) P3TAA–P3AT, (f) P3TAA–PT and (g) bare TiO_2 film with the electrolyte.

Figure 6 shows the photocurrent–voltage responses of TiO_2 film with different polymer dyes. While curves (a), (b), (c), (f), (i) and (j) show the photoresponses of the cells fabricated with P3TAA, P3TAA–P3TMA, P3TAA–P3MT, P3TAA–P3AT, P3TAA–PT and P3TAA–PPy respectively, with the ionic liquid in the electrolyte; curves (d), (e), (g), (h), (k) and (l) respectively show the photoresponses of the above cells without the ionic liquid. Together with the dark (not shown here) and the photo *I*–*V* responses, it is evident that the devices have good junction properties. The corresponding values obtained for the main parameters such as short (J_{sc}), (V_{oc}), FF and η are shown in Table 1. As seen from Figure 6 and Table 1, the addition of MHImI drastically enhances the overall performances of the cells. This might be attributed to the increase in electron diffusion in the nanoporous TiO_2 electrodes and the improvement in the physical properties such as conductivity, stability, etc. of the polymers in the presence of an ionic liquid. Unexpectedly, the cell sensitized with P3TAA showed the highest photocurrent, voltage, fill factor and conversion efficiency compared to the other cells. It should be noted that after introducing both the electrolyte and the ionic liquid into the cells, suffi-

Table 1. Estimated physical parameters of the polymers with their photoresponses in photovoltaic cells

	λ_{max} (nm)	Band gap	Band position HOMO	Band position LUMO	Without ionic liquid J_{sc} (mA cm^{-2})	Without ionic liquid V_{oc} (mV)	Without ionic liquid FF (%)	Without ionic liquid η (%)	With ionic liquid J_{sc} (mA cm^{-2})	With ionic liquid V_{oc} (mV)	With ionic liquid FF (%)	With ionic liquid η (%)
P3TAA	417	2.39	5.29	2.90	3.03	453	57	0.79	4.35	472	59	1.21
P3TAA–P3TMA	426	2.48	5.07	2.59	2.65	408	52	0.56	3.29	407	57	0.76
P3TAA–P3MT	415	2.50	5.00	2.50	2.88	422	58	0.70	3.12	423	58	0.76
P3TAA–P3AT	411	2.57	5.04	2.47	2.64	306	39	0.31	2.97	314	55	0.51
P3TAA–PT	391	2.46	5.01	2.55	1.51	300	59	0.28	2.25	307	61	0.42
P3TAA–PY	420	2.47	5.03	2.56	1.69	374	51	0.32	1.85	402	56	0.41

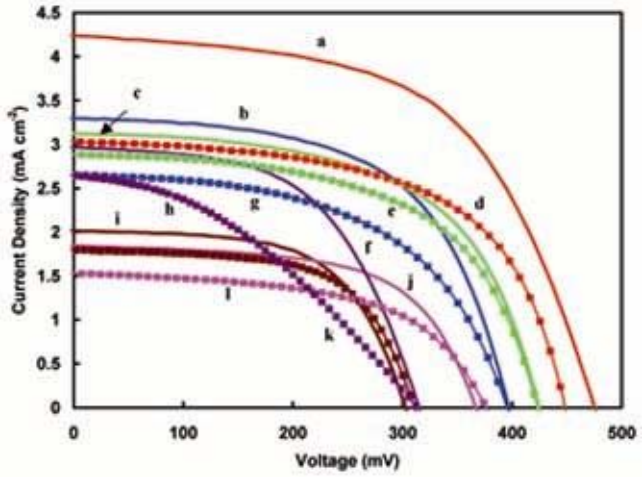

Figure 6. Photocurrent–voltage response of TiO_2 film with different polymer dyes. Curves (a), (b), (c), (f), (i) and (j) show the photoresponse of the cells fabricated with P3TAA, P3TAA–P3TMA, P3TAA–P3MT, P3TAA–P3AT, P3TAA–PT and P3TAA–PPy respectively, with the ionic liquid in the electrolyte. Curves (d), (e), (g), (h), (k) and (l) respectively show the photoresponse of the above cells without the ionic liquid.

cient time is required for them to penetrate the electrolytes to reach the bottom of the film in order to obtain high efficiency for the cells. It was also observed from the above values that the quantum efficiency decreased with increasing film thickness, probably due to decreasing electron collection and increasing electron recombination with increase in thickness, as explained by a finite diffusion length of the solar cells. Another reason for the lower V_{oc} of these cells than the ruthenium dye-sensitized cells, may be related to the shift in the conduction band edge of the inorganic semiconductor due to the protonation of the surface by the polymer[19]. Preliminary tests on the stability under continued illumination with a 15 W Osram Day Light lamp at intensity of 325 Wm^{-2} (the spectrum of the lamp matches the absorption spectrum of the polymer) for two weeks were carried out with poor sealing, and it was observed that the cells fabricated with MHImI showed improved stability with almost no change in efficiency during the above period. However, for longer stability, perfect sealing should be done to avoid contact with the moisture. Even though these efficiency values seems to be low, they are significant and even higher than the values reported with several dyes and organic sensitizers such as mercurochrome[24] (η = 2.5%), polythiophenes[14] (IPCE = 0.5–1), cyanadin[25] (η < 1%), perylene derivatives[26] (η < 1%), etc.

Conclusion

In this study we explored the potentialities of using co-polymers with carboxylic moities in polymer-sensitized photoelectrochemical devices. Polymer-sensitized, nanocrystalline, photo-electrochemical devices were successfully fabricated with higher efficiencies than the reported devices with conducting polymers as sensitizers. Even though these polymer-sensitized solar cells produce high open-circuit voltage, short-circuit photocurrent, fill factor and the overall efficiency are much lower than those available from inorganic sensitizers. The co-polymer we have synthesized could not absorb light in the longer wavelengths. However, there is a possibility of improving the light harvesting by synthesizing some co-polymers with P3TAA having COOH groups and some polymers with red-absorbing moities. Further improvements are presently being investigated.

1. Regan B. O. and Grätzel, M., A low-cost, high-efficiency solar cell based on dye-sensitized colloidal TiO_2 films. *Nature*, 1991, **353**, 737–740.
2. Nazeeruddin, M. K. *et al*., Conversion of light to electricity by cis-X2bis(2,2′-bipyridyl-4,4′-dicarboxylate)ruthenium(II) charge-transfer sensitizers (X = Cl^-, Br^-, I^-, CN^- and SCN^-) on nanocrystalline titanium dioxide electrodes. *J. Am. Chem. Soc.*, 1993, **115**, 6382–6390.
3. Chen, J., Too, C. O., Burrel, A. K., Collis, G. E., Officer, D. L. and Wallace, G. G., Photovoltaic devices based on poly(bisterthiophenes) and substituted poly(bisterthiophene). *Synth. Met*., 2003, **137**, 1373–1374.
4. Smestad, G., Bignozzi, C. and Argazzi, R., Testing of dye sensitized TiO_2 solar cells I: Experimental photocurrent output and conversion efficiencies. *Sol. Energy Mater. Sol. Cells*, 1994, **32**, 259–272.
5. Hara, K., Sayama, K., Ohga, Y., Shinpo, A., Suga, S. and Arakawa, H., A coumarin-derivative dye sensitized nanocrystalline TiO_2 solar cell having a high solar-energy conversion efficiency up to 5.6%. *Chem. Commun*., 2001, **6**, 569–570.

6. Gazotti, W. A., Girotto, E. M., Nogueira, A. F. and DE Paoli, M. A., Solid-state photoelectrochemical cell using a polythiophene derivative as photoactive electrode. *Sol. Energy Mater. Sol. Cells*, 2001, **69**, 315–323.
7. Huynh, W. U., Dittmer, J. J. and Alivisatos, A. P., Hybrid nanorod–polymer solar cells. *Science*, 2002, **295**, 2425–2427.
8. Roman, L. S. and Inganäs, O., Charge carrier mobility in substituted polythiophene-based diodes. *Synth. Met*., 2001, **125**, 419–422.
9. Grant, C. D., Schwartzberg, A. M., Smestad, G. P., Kowalik, J., Tolbetrt, L. M. and Zhang, J. Z., Characterization of nanocrystalline and thin film TiO_2 solar cells with poly(3-undecyl-2,2′-bithiophene) as a sensitizer and hole conductor. *J. Electroanal. Chem*., 2002, **522**, 40–48.
10. Smestad, G. P. *et al.*, A technique to compare polythiophene solid-state dye sensitized TiO_2 solar cells to liquid junction devices. *Sol. Energy Mater. Sol. Cells*, 2003, **76**, 85–105.
11. Kim, B. S., Chen, L., Gong, J. and Osasa, Y., Titration behavior and spectral transitions of water-soluble polythiophene carboxylic acids. *Macromolecules*, 1999, **32**, 3964–3969.
12. Senadeera, G. K. R., Nakamura, K., Kitamura, T., Wada, Y. and Yanagida, S., Fabrication of highly efficient polythiophene-sensitized metal oxide photovoltaic cells. *Appl. Phys. Lett*., 2003, **83**, 5470.
13. Yanagida, S., Senadeera, G. K. R., Nakamura, K., Kitamura, T. and Wada, Y., Polythiophene-sensitized TiO_2 solar cells. *J. Photochem. Photobiol. A: Chem*., 2004, **166**, 75–80.
14. Senadeera, G. K. R., Kitamura, T., Wada, Y. and Yanagida, S., Photosensitization of nanocrystalline TiO_2 films by a polymer with two carboxylic groups, poly(3-thiophenemalonic acid). *Sol. Energy Mater. Sol. Cells*, 2005, **88**, 315–322.
15. Senadeera, R., Fukuri, N., Saito, Y., Kitamura, T., Wada, Y. and Yanagida, S., Volatile solvent free solid state polymer sensitized TiO_2 solar cells with poly(3,4-ethylenedioxythiophene) as a hole transporting medium. *Chem. Commun*., 2005, **17**, 2259–2261.
16. Senadeera, G. K. R., Kitamura, T., Wada, Y. and Yanagida, S., Deposition of polyaniline via moleculer self assembly on TiO_2 and its uses in as a sensitizer in solid sate solar cells. *J. Photochem. Photobiol. A: Chem*., 2004, **164**, 61–66.
17. Kubo, W., Kambe, S., Nakade, S., Kitamura, T., Hanabusa, K., Wada, Y. and Yanagida, S., Photocurrent-determining processes in quasi-solid-state dye-sensitized solar cells using ionic gel electrolytes. *J. Phys. Chem. B*, 2003, **107**, 4374–4381.
18. Lu, W. *et al.*, Use of ionic liquids for p-conjugated polymer electrochemical devices. *Science*, 2002, **297**, 983–987.
19. Nazeeruddine, K. *et al.*, Acid–base equilibria of (2,2′-bipyridyl-4,4′-dicarboxylic acid)ruthenium(II) complexes and the effect of protonation on charge-transfer sensitization of nanocrystalline titania. *Inorg. Chem*., 1999, **38**, 6298–6305.
20. Bredas, J. L., Silbey, R., Boudreaux, D. S. and Chance, R. R., Chain-length dependence of electronic and electrochemical properties of conjugated systems: Polyacetylene, polyphenylene, polythiophene, and polypyrrole. *J. Am Chem. Soc*., 1983, **105**, 6555–6559.
21. Silverstien, R. M. and Webster, F. X., *Spectroscopic Identification of Organic Compounds*, John Wiley, NY, 1998, 6th edn.
22. Hsieh, K. H., Ho, K. S., Wang, Y. Z., Ko, S. D. and Fu, S. C., Miscibility of poly(thiophene-3-acetic acid) and poly(ethylene oxide). *Synth. Met*., 2001, **123**, 217–224.
23. Chen, T. A., Wu, X. and Rieke, R. D., Regiocontrolled synthesis of poly(3-alkylthiophenes) mediated by Rieke zinc: Their characterization and solid-state properties. *J. Am. Chem. Soc*., 1995, **117**, 233–244.
24. Hara, K., Horiguchi, T., Kinoshita, T., Sayama, K., Sugihara, H. and Arakawa, H., Highly efficient photon to electron conversion with mercurochrome sensitized nanoporous oxide semiconductor solar cells. *Sol. Energy Mater. Sol. Cells*, 2000, **64**, 115–134.
25. Tennakone, K., Kumarasinghe, A. R., Kumara, G. R. R. A., Wijayanthe, K. G. U. and Sirimanne, P. M., Nanoporous TiO_2 photoanode sensitized with the flower pigment cyaniding. *J. Photochem. Photobiol*.: *Chem. A*, 1997, **108**, 193–195.
26. Ferrere, S., Zaban, A. and Gregg, B. A., Dye sensitization of nanocrystalline tin oxide by perylene derivatives. *J. Phys. Chem. B*, 1997, **101**, 4490–4493.

ACKNOWLEDGEMENTS. We thank the National Science Foundation of Sri Lanka for financial assistance and The Academy of Sciences for the Developing World.

Received 4 September 2007; revised accepted 16 July 2008